Compensating for Orientation Mismatch in Robust WiFi Localization Using Histogram Equalization

Shih-Hau Fang, *Senior Member, IEEE*, Chu-Hsuan Wang, and
Yu Tsao, *Member, IEEE*

***Abstract*—The performance of Wi-Fi positioning systems degrades severely when the user orientation differs between locating and training phases. This paper proposes a novel approach based on histogram equalization to compensate for an orientation mismatch in robust Wi-Fi localization. The proposed method involves converting the temporal-spatial radio signal strength into a reference function (i.e., equalizing the histogram). By using equalized signals, the proposed algorithm improves the robustness of location estimation even in the presence of mismatch orientation. The advantages of the proposed algorithm over traditional methods are that the assumption of user behavior is not required and a digital compass does not need to be embedded on a mobile device. Experiments conducted in Wi-Fi networks demonstrated the effectiveness of the proposed algorithm. The results show that the proposed algorithm outperforms the orientation classifier method and provides comparable positioning accuracy to the compass-assisted approach.**

***Index Terms*—Histogram equalization (HEQ), mobile positioning, received signal strength (RSS), user orientation, Wi-Fi**

I. Introduction

LOCATION awareness has become a crucial concern for various mobile applications [1]–[7]. Recently, numerous studies have addressed location estimation by using existing Wi-Fi infrastructure to compensate for the weakness of the Global Positioning System (GPS) in urban areas and indoor environments [8]–[11]. Because of the frequent deployment of access points (APs), Wi-Fi-based localization has gained considerable attention over the last several years, and the received signal strength (RSS) is commonly adopted as a positioning characteristic [12]–[14]. Among the various Wi-Fi positioning systems, the fingerprinting-based approach, in which the user's location is estimated by matching online RSSs with the values pre-stored in a radio map, is one of the most feasible solutions [15]–[18]. Because this approach provides a high positioning accuracy in a GPS-less environment, researchers have recently proposed various fingerprinting-based localization algorithms [19]–[21].

Although Wi-Fi-based localization shows great promise, a key challenge in real-time location estimation is managing the robustness from various perspectives [22], [23]. For example, researchers have addressed heterogeneity in the hardware of Wi-Fi devices [24]–[26]. Previous studies have designed secure location systems that can identify malicious network attacks and reject them from the positioning system [27]–[31]. Several studies have investigated noise and multipath distortion [32]–[38]. Robust pattern matching, outliers removement, and data-overfitting problems have also been discussed in the literature [39]–[44].

Radio irregularity is a common occurrence in wireless environments [40], [45], [46]. The performance of fingerprinting-based localization systems degrades severely when radio environments between training and testing RSSs differ from each other [47]. One type of radio mismatch is caused by the different user orientations. Users tend to carry mobile devices in front of them so that they can view the displays and use the touch screen. However, the human body consists of more than 50% water and, hence, might block the transmission of 2.4 GHz Wi-Fi radios [48]. Researchers have performed experiments regarding the impact of user/device orientation on RSS. Previous studies have acknowledged this orientation problem and have indicated that RSS varies substantially depending on the user's orientation, even at a fixed location [42], [49]. However, in a fingerprinting-based system, the mismatch between training and locating orientations makes it difficult to accurately determine the location based on RSS patterns. This severe problem is referred to as "orientation mismatch."

To overcome this problem, [50] proposed a compass-assisted approach in which the testing RSS is matched according to the orientation-matched radio map only, rather than the entire database. A similar approach was presented in [51] and [52], in which fingerprinting is extended with orientation information. These approaches effectively reduce the orientation mismatch effect; however, they require prior orientation data to enrich the radio map and real-time feedback from a digital compass. Although current high level smartphones can be equipped with compass sensing functions that provide real-time user orientation, reconstructing a radio map for every possible orientation is extremely time consuming and infeasible.

This study proposes a novel approach based on histogram equalization (HEQ) to compensate for an orientation mismatch in robust Wi-Fi localization. The basic idea is to convert the probability density function of original RSS vectors into a reference probability density function. Specifically, the proposed algorithm transforms the histogram of each component of the temporal-spatial Wi-Fi radio into that of a reference (i.e., it equalizes the histogram). By using the equalized RSSs, the proposed algorithm is capable of improving the robustness

Shih-Hau Fang and Chu-Hsuan Wang are with the Department of Electrical Engineering and Innovation Center for Big Data and Digital Convergence, Yuan Ze University, Taoyuan, Taiwan. Yu Tsao is with the Research Center for Information Technology Innovation, Academia Sinica, Taipei, Taiwan. (Email: shfang@saturn.yzu.edu.tw, s1008503@mail.yzu.edu.tw, and yu.tsao@citi.sinica.edu.tw)

of location estimation, even in the presence of mismatch orientation. Compared with traditional methods, the proposed algorithm is easy to implement in practical applications. The proposed algorithm does not involve assumptions regarding user behavior, and the only assumption is that the effect of orientation mismatch causes a certain transformation of the RSS representation space.

The proposed algorithm was applied in an indoor Wi-Fi environment, and RSSs were collected from various user orientations. On-site experiments demonstrated the effectiveness of the proposed algorithm in compensating for the orientation mismatch. Results showed that the proposed approach outperforms the orientation classifier in reducing the mean positioning errors between 16% and 42% in various mismatch conditions. The results also demonstrated that the proposed algorithm provides a comparable positioning accuracy to that of the compass-assisted approach.

II. Proposed Indoor Positioning System

A. Problem Statement

A probabilistic location algorithm estimates the likelihood of observations for all candidate locations and selects the one having maximum likelihood as the result. This can be formulated as

$$\begin{aligned} j^* &= arg\max_j P(\Lambda_j|S) \\ &= arg\max_j \frac{P(S|\Lambda_j)P(\Lambda_j)}{P(S)} \\ &= arg\max_j P(S|\Lambda_j) \\ &= arg\max_j \prod_{i=1\ldots M} P(s_i|\Lambda_j), \end{aligned} \tag{1}$$

where j is the index of the reference location, j^* is the maximum-likelihood estimation, Λ_j is the model parameters of the j-th reference location, S is the RSS observation, and s_i is the i-th element of S. In Eq. (1), $P(\Lambda_j)$ is assumed to be equal $\forall j$ and $P(S)$ does not affect the decision result. This approach is widely-used for indoor WLAN location fingerprinting systems. However, this positioning algorithm is sensitive to orientation mismatch. Assuming Y is an orientation-mismatched observation, this process becomes

$$\begin{aligned} j^{**} &= arg\max_j P(\Lambda_j|\mathrm{Y}) \\ &= arg\max_j \int P(\Lambda_j|\mathrm{Y},\mathrm{S})P(\mathrm{S}|\mathrm{Y})dS \\ &= arg\max_j \int P(\Lambda_j|\mathrm{S})P(\mathrm{S}|\mathrm{Y})dS \\ &= arg\max_j \int \frac{P(S|\Lambda_j)P(\Lambda_j)}{P(S)}P(\mathrm{S}|\mathrm{Y})dS \\ &= arg\max_j \prod_{i=1\ldots M}\int \frac{P(s_i|\Lambda_j)}{P(s_i)}P(s_i|\mathrm{Y})ds_i, \end{aligned} \tag{2}$$

where j^{**} is the new estimation in this mismatched scenario. We assume that s_i is only dependent on the current mismatched observation, $P(s_i|\mathrm{Y}) = P(s_i|y_i)$. Based on the point estimate, we assume $P(s_i|y_i) = \delta(s_i - \widehat{s_i}(y_i))$, where $\widehat{s_i}(y_i) = F(y_i)$, $\widehat{s_i}$ denotes the orientation-matched signal, $F(\cdot)$ denotes a transformation function, and $\delta(\cdot)$ is a Kronecker delta function. The new estimation in Eq. (2) can be re-written as:

$$j^{**} = arg\max_j \prod_{i=1\ldots M} P(\widehat{s_i}(y_i)|\Lambda_j) \tag{3}$$

Comparing Eq. (3) with Eq. (1), we can observe the difference between the likelihood formulations, i.e., $j^{**} \neq j^*$. The goal of the robust location estimation is to make j^{**} approaches j^*. That is, $\widehat{s_i}(y_i) = F(y_i) \rightarrow s_i$. However, designing the transformation function that achieves the above is difficult without a set of paired training and testing data.

Now consider a rather naive assumption that the distributions of training data and observation data are both Gaussians and parameterized by $\{\mu_\mathrm{S}, \sigma_\mathrm{S}\}$ and $\{\mu_\mathrm{Y}, \sigma_\mathrm{Y}\}$, respectively. To estimate a transformation function making two distributions close, the simplest way is to match the mean of these two distributions, which can be done in two types of implementation: direct approach and indirect approach. For the direct approach, testing RSSs are transformed to match training data directly; for the indirect approach, both training and testing data are transformed to a same reference distribution. In this case, the transformation function is $F(y_i) = y_i - \mu_\mathrm{Y} + \mu_\mathrm{S}$ for the direct approach, whereas we perform $F(y_i) = y_i - \mu_\mathrm{Y}$ and $F(s_i) = s_i - \mu_\mathrm{S}$ for the indirect approach. If we consider normalize both mean and variance, the direct approach applies $F(y_i) = (y_i - \mu_\mathrm{Y})\frac{\sigma_S}{\sigma_Y} + \mu_\mathrm{S}$, and the indirect approach performs $F(y_i) = (y_i - \mu_\mathrm{Y})/\sigma_\mathrm{Y}$ and $F(s_i) = (s_i - \mu_\mathrm{S})/\sigma_\mathrm{S}$. The direct approach transforms the testing data to share the same mean and variance with the training data, while the indirect approach transforms both training and testing data to the same zero mean and unit variance Gaussian distribution.

However, in realistic situations, the impact of user orientation mismatch on the RSS values may not be linear, and the training and testing distributions are not necessary Gaussians. Moreover, more accurate matching is to normalize higher statistical moments apart from the mean and variance. This motivates us to adopt histogram equalization to overcome this problem. The histogram equalization described here equalizes all the moments of the probability distribution to those of the reference probability distribution. Therefore, this procedure can be considered to be an extension of mean and variance normalization.

Traditional works assume the availability of orientation information during the offline and online phases while dealing with the mismatch problem [50]–[53]. In other words, these methods are based on the orientation-aware radio map and the likelihood becomes

$$j^{***} = arg\max_j \prod_{i=1\ldots M} P(s_i^{(o)}|\Lambda_j^{(o)}) \tag{4}$$

where o indicates the current users orientation, $s_i^{(o)}$ means the current RSSs under o, and Λ_j^o represents the model parameters estimated from the data with the same orientation o. Because the orientation information is given, j^{***} extremely approaches j^* and such a compass-assisted approach can be

regarded as a performance upper bound. Feng et al. [53], [54] combines affinity propagation [55] and compressive sensing to improve the positioning accuracy, where the current user orientation is ignored. These approaches effectively reduce the orientation mismatch effect; however, they require prior orientation data to enrich the radio map and real-time feedback from a digital compass.

Although current high levels smartphones can be equipped with compass sensing functions that provide real-time user orientation, reconstructing a radio map for every possible orientation is extremely time consuming and infeasible. The goal of this paper aims at alleviating the impact of orientation mismatch without the need of orientation information from either radio map or embedded sensors. Liao et al. [56] proposed the orientation classifier approach, which is used to predict the user's orientation based on the moving trajectory and RSS variations. However, the effectiveness of this method depends on the assumption that a user moves at a constant speed in a fixed direction. This assumption could be erroneous, and modeling the orientation process is difficult due to the random user behavior.

B. Theoretical Foundation of Histogram Equalization

HEQ has been recognized as an effective digital image processing method for optimizing the dynamic grey-level ranges and improving the brightness and contrast [57]. The purpose of HEQ is to provide a transformation that converts the probability density function of an original variable into a reference probability density function. In other words, the transformation equalizes the histograms [58]. In addition to digital image processing, HEQ has also been introduced to the field of speech processing [58]–[60].

As presented in Section II-A, this study proposes to use HEQ to reduce the mismatch by equalizing all the moments of the probability distributions of training and testing data. Now we assume $r_i = F(x_i)$, where r_i and x_i, respectively, denote the i-th reference and original data. Let $p_r(r)$ and $p_x(x)$ denote the density functions of reference and original data, respectively, and the goal of HEQ is to compute $F(\cdot)$ that converts $p_x(x)$ to approach $p_r(r)$ [57], [58]. The derivation of HEQ is provided below.

First, we have:

$$p_r(r) = p_x\left(G\left(r\right)\right)\frac{\partial G\left(r\right)}{\partial r} \tag{5}$$

where $G(\cdot)$ is the inverse function of $F(\cdot)$. Note that we make $F(\cdot)$ invertible by using probabilistic one-to-one transformation functions $C_r(\cdot)$ and $C_x(\cdot)$. The relationship between the cumulative probability density functions (CDFs) associated with these probability distributions is given by

$$\begin{aligned} C_x(x) &= \int_{-\infty}^{x} p_x(x^{'})dx^{'} \\ &= \int_{-\infty}^{F(x)} p_x(G(r^{'}))\frac{\partial G(r^{'})}{\partial r^{'}}dr^{'} \\ &= \int_{-\infty}^{F(x)} p_r(r^{'})dr^{'} \\ &= C_r(F(x)) \end{aligned} \tag{6}$$

where $C_r(F(x))$ and $C_x\left(x\right)$ are CDFs of the reference and original distribution, respectively. The transformation

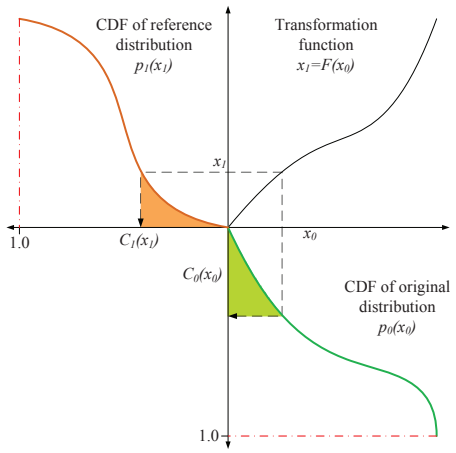

Fig. 1. The main idea of the histogram equalization procedure [58].

$r = F(x)$, which converts distribution $p_x(x)$ into reference distribution $p_r(r)$, also converts the cumulative probability $C_x\left(x\right)$ into $C_r\left(r\right)$. Hence, the transformation function $F(\cdot)$ converting $p_x(x)$ into $p_r(r)$ is expressed as

$$r = F\left(x\right) = C_r^{-1}\left[C_x\left(x\right)\right] \tag{7}$$

where C_r^{-1} denotes the inverse function of the CDF $C_r\left(r\right)$, specifying the value r that corresponds to a certain cumulative probability.

Considering practical implementations, the cumulative histograms are typically used because the number of observations is finite. Therefore, the procedure is referred to as HEQ in the literature. The main concept of HEQ is illustrated in Fig. 1 [58], where the green and orange integral areas indicate the CDFs of x and r, respectively. The black line represents the transformation by which the algorithm equalizes the histograms $C_x(x) = C_r(r)$, as indicated in Eq. 7.

HEQ can be implemented in two manners: direct and indirect. In the former, the distribution of the training data is used as the reference distribution, and the HEQ is applied to only convert the probabilistic density of testing data to match the one of training data. In the latter, we transform the probabilistic densities of both training and testing data to a reference distribution. The reference distribution is defined in advance, and the Gaussian distribution is a common choice. The following section describes how it can be adapted for Wi-Fi indoor localization with details.

C. Proposed Indoor Positioning Algorithm

1) Offline Phase: The proposed indoor WLAN positioning system consists of two phases: offline and online. In the offline phase, RSS readings from Wi-Fi APs at reference positions are collected to build a database, called a radio map. The raw RSS data are denoted by $\psi_{i,j}^{(o)}[\tau]$, and indicate the τ-th RSS value measured from the i-th AP at the j-th reference location, with orientation o. The offline-constructed radio map can then be spanned and represented by $\mathbf{\Psi}$ as

$$\mathbf{\Psi}^{(o)} = \begin{pmatrix} \psi_{1,1}^{(o)}[\tau] & \psi_{1,2}^{(o)}[\tau] & \cdots & \psi_{1,N}^{(o)}[\tau] \\ \psi_{2,1}^{(o)}[\tau] & \psi_{2,2}^{(o)}[\tau] & \cdots & \psi_{2,N}^{(o)}[\tau] \\ \vdots & \vdots & \ddots & \vdots \\ \psi_{M,1}^{(o)}[\tau] & \psi_{M,2}^{(o)}[\tau] & \cdots & \psi_{M,N}^{(o)}[\tau] \end{pmatrix} \quad (8)$$

where M is the number of APs, N is the number of reference locations, o is the measured orientations from an embedded digital compass, $\tau = 1, \ldots, Q$ is the index of temporal RSS samples, and Q is the number of samples for each raw RSS data. The row vector of $\mathbf{\Psi}$ indicates the spatial RSS vectors over N reference locations with Q temporal length in the target environment. The column vector of $\mathbf{\Psi}$, representing the M dimensional RSS training samples for the j-th reference location, can be represented as

$$\Psi_j = [\psi_{1,j}^{(o)}, \psi_{2,j}^{(o)}, \cdots \psi_{M,j}^{(o)}]^{\mathrm{T}}. \quad (9)$$

Incorporating the orientation parameter is a generalization of the RSS collection procedure. This value may be missing for certain indoor positioning systems. It represents the difficulty of determining the location based on a history of RSS patterns $\mathbf{\Psi}$. The goal of the proposed algorithm is to achieve robust location estimation in the presence of orientation mismatch without assistance from a digital compass. That is, the proposed algorithm allows the attribute o to be ignored when the orientation is unavailable because of the lack of a digital compass.

2) Online phase: During the online phase, a mobile device requests positioning services by using the online RSSs from M APs. Using similar notations, the real-time measurements can be represented as

$$\mathbf{\Psi}_r^{(o)} = \begin{pmatrix} \psi_{1,r}[1], \psi_{1,r}[2], \ldots, \psi_{1,r}[q] \\ \psi_{2,r}[1], \psi_{2,r}[2], \ldots, \psi_{2,r}[q] \\ \vdots \\ \psi_{M,r}[1], \psi_{M,r}[2], \ldots, \psi_{M,r}[q] \end{pmatrix}_{M \times q} \quad (10)$$

where the location index r and the orientation attribute are unknown, representing that a digital compass is unnecessary in the proposed algorithm. In this study, the real-time measurements $\mathbf{\Psi}_r^{(o)}$ is called as a temporal-spatial radio, which consists of q temporal RSSs from M APs. HEQ was then applied to each component of this temporal-spatial measurement matrix. The first step is to reshape $\mathbf{\Psi}_r^{(o)}$ into a vector form as follows:

$$\mathbf{\Phi} = [\phi_1, \phi_2, \ldots, \phi_q, \phi_{q+1}, \ldots, \phi_{M \cdot q}]. \quad (11)$$

Equation (11) is used to reshape the array in (10) into a row vector $\mathbf{\Phi}$ with $M \cdot q$ elements, where $\phi_1 = \psi_{1,r}[1]$, $\phi_q = \psi_{1,r}[q]$, $\phi_{q+1} = \psi_{2,r}[1]$, and $\phi_{M \cdot q} = \psi_{M,r}[q]$.

For simplification, a reorganized sequence S consisting of $M \cdot q$ elements of a test RSS component in ϕ_r is then defined as

$$S = [s_1, s_2, \ldots, s_{M \cdot q}]. \quad (12)$$

The difference between Eq. 12 and Eq. 11 lies in the order statistics, which can be represented as

$$\phi_{T(1)} \leq \phi_{T(2)} \leq \cdots \leq \phi_{T(a)} \leq \cdots \leq \phi_{T(M \cdot q)} \quad (13)$$

where $T(\cdot)$ denotes the original index of the test RSS components in such a way that $s_a = \phi_{T(a)}$. Given S, an estimate of the equalized RSS component based on Eq. (7) is obtained using

$$\hat{s}_i = F(s_i) = C_{ref}^{-1}[C_S(s_i)] \quad (14)$$

where C_{ref}^{-1} is the inverse of the reference CDF, C_S represents the CDF of the sequence S, F is the equalized transformation, and $\hat{s}_i$ is the i-th equalized RSS. One can compute $C_S(s_i)$ by the empirical distribution function which is the number of observations less than or equal to s_i divided by the total numbers.

The selection of reference distribution C_{ref} for equalization has been discussed in [57], [58], and two widely-used methods are adopted in this study: Gaussian distribution (indirect approach) and training distribution (direct approach). First, while adopting a typical Gaussian distribution as a reference (called Gaussianization) in the indirect approach, the inverse CDF can be expressed as

$$C_{ref}^{-1}(z) = \left[\Phi\left(\frac{z-\mu}{\sigma}\right)\right]^{-1} = [\Phi(z')]^{-1} \quad (15)$$

where z is a reference Gaussian variable with mean μ and standard deviation σ. The variable z' is the normalized Gaussian variable and Φ is an error function expressed as

$$\Phi(z') = \frac{1}{\sqrt{2\pi}} \int_{-\infty}^{z'} e^{-u^2/2} du \quad (16)$$

Next, the training distribution means estimating CDF from the training radio map as reference for equalization. This direct approach can be viewed as an non-parametrical version of the Gaussian distribution in which the shape is estimated empirically. The only requirement is sufficient temporal-spatial radio data to calculate the training distribution. Note that the training distribution can be stored in the offline stage such that the equalization does not require additional real-time estimation process.

3) Localization Using the Equalized RSS: After equalizing the online temporal-spatial RSSs, the equalized components are adopted for positioning using a probabilistic approach. This method involves mapping the equalized RSSs to a physical location by interpolation using the normalized likelihood value:

$$\hat{L} = \sum_{j=1}^{N} L_j \cdot \hat{P}_j \quad (17)$$

where L_j represents the coordinates of the j-th reference location and $\hat{P}_j$ is a normalized likelihood with respect to all posterior probabilities as

$$\hat{P}_j = \frac{P(\hat{\mathbf{s}}|L_j)}{\sum_{j=1}^{N} P(\hat{\mathbf{s}}|L_j)} \quad (18)$$

In Eq. 18, $P(\hat{\mathbf{s}}|L_j)$ represents the likelihood of measuring $\hat{\mathbf{s}}$ at the j-th reference location, where $\hat{\mathbf{s}} = [\hat{s}_1, \hat{s}_2, \ldots, \hat{s}_M]^{\mathrm{T}}$ are the equalized RSSs from M APs. Assuming the equalized signals are modeled as Gaussian distributions, the statistical parameters, including a mean vector $\hat{u}_j \in \Re^{M*1}$ and a covariance matrix $\Omega_j \in \Re^{M*M}$, are calculated and stored for each L_j during the off-line phase using

$$\hat{u}_j = \frac{1}{q}\sum_{\tau=1}^{q} \hat{\Psi}_j[\tau] \tag{19}$$

$$\Omega_j = E[(\hat{\Psi}_j - \hat{u}_j)(\hat{\Psi}_j - \hat{u}_j)^{\mathrm{T}}] \tag{20}$$

where $\hat{\Psi}_j[\tau]$ indicates the τ-th equalized training RSS sample at the j-th reference location and the notation E represents the average over q temporal samples. HEQ was applied as the Wi-Fi radio representation for both online measurements and offline training RSSs. This procedure is required for the likelihood computation. The equalized training RSS samples can be obtained using Eq. 14 as follows:

$$\hat{\Psi}_j = C_{ref}^{-1}\left[C_{\Psi_j}(\Psi_j)\right] \tag{21}$$

where the reference probabilistic distribution is the same as that used in the on-line phase. If one selects a typical Gaussian as reference probabilistic distributions, C_{ref}^{-1} can be obtained using Eq. 15. If one selects the training distribution as reference, estimating CDF from the training radio map is required to compute C_{ref}^{-1} for equalization. $C_{\Psi_j}(\Psi_j)$ can be empirically estimated by dividing the number of observations less than a certain value by the total numbers. After estimating the statistical parameters based on the equalized RSSs, the likelihood weights $P(\hat{\mathbf{s}}|L_j)$ in Eq. 18 can be calculated as follows:

$$P(\hat{\mathbf{s}}|L_j) = \prod_{m=1}^{M} \frac{1}{\sqrt{2\pi \cdot \Omega_j(m,m)}} \exp\left(\frac{-(\hat{s}_m - \hat{u}_j(m))^2}{2\Omega_j(m,m)}\right) \tag{22}$$

where $\hat{u}_j(m)$ is the m-th element of the mean vector $\hat{u}_j$ and the APs are assumed to be uncorrelated. Although assuming the diagonal matrix could be erroneous, this is widely used for implementing the probabilistic approach due to some practical constraints, such as insufficient training data. In this study, the amount of data is not sufficient to train an accurate full matrix and thus, a diagonal matrix is used for the location estimation. We note that although histogram estimation is required for this algorithm, it is easier than traditional methods, which require either a digital compass or an assumption of user behavior. The effect of orientation mismatch is assumed to cause a certain transformation of the RSS representation space. Therefore, the proposed algorithm equalizes RSSs to prevent the performance degradation caused by mismatch orientation. During positioning, HEQ is implemented for training data and real-time measurements in parallel, and the device coordinates are estimated by mapping the equalized RSSs to the physical location using the normalized likelihood values. While performing the nonlinear transformation, this approach preserves the ranking of RSSs instead of the numerical RSS values. When RSS values are reliable, such as perfectly follow the radio propagation model, the transformation may loss some location information and the side effect is possible in some clean environments.

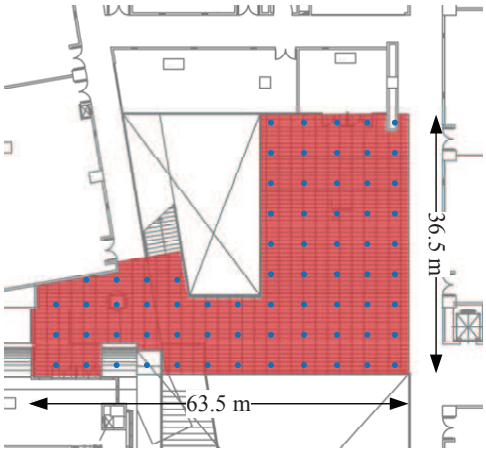

Fig. 2. Part of the fourth floor plane of the test-bed building, where we performed the experiments.

III. Experimental Results and Analysis

A. Experimental Setup

This study involved experiments conducted on the fourth floor of the telecommunications building at Yuan-Ze University. Fig. 2 shows where the experiments were performed. The size of the test-bed was 63.5 (m) $\times$ 36.5 (m) and 30 detectable APs were present in the environment (M=30). An Asus laptop with Windows XP and NetStumbler network software were used to gather Wi-Fi RSSs from the APs. The RSS readings were recorded at 70 reference locations (N=70), separated by a distance of 1.2 to 2 m and arranged in four orientations, to build the radio map for the indoor positioning system. The testing samples were measured at 30 distinct locations in this test field. To evaluate the orientation effects, users orientated in four directions, north, east, south, and west and the corresponding RSS values were recorded. At each reference location, 50 RSS samples (Q=50) were recorded for each orientation. A Gaussian distribution with zero mean and unity variance was used as the reference distribution. HEQ was applied to each component of the temporal-spatial Wi-Fi radio for both offline and online phases. To obtain the transformation of each component, the cumulative histogram was estimated by considering 100 uniform intervals between $u_i \pm 4\sigma_i$, where u_i and σ_i are the mean and standard deviation of the i-th component of the reshaped RSS vector, respectively.

B. Performance Evaluation

First, Fig. 3 shows the distribution of RSS measurements from four orientations, at the same location, from the same AP. The lines indicate that the average RSS values from north, east, south, and west were -57.7, -56.6, -63.5, and -61.1 dBm, respectively. This figure clearly reveals the changing RSS patterns problem caused by the user orientation variation. It indicates the difficulty of accurately determining the location

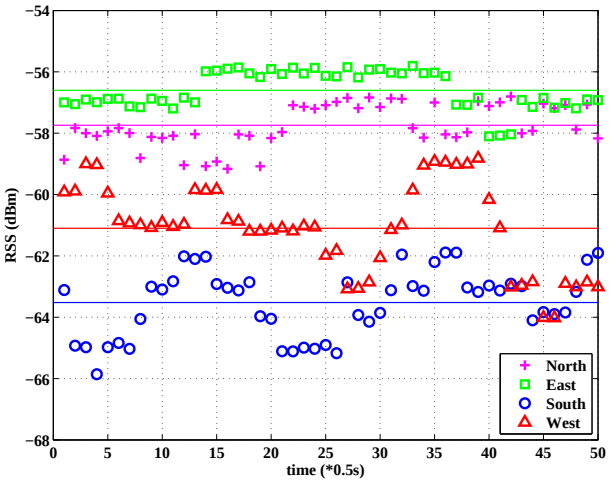

Fig. 3. The RSS distributions from the same AP with different orientations.

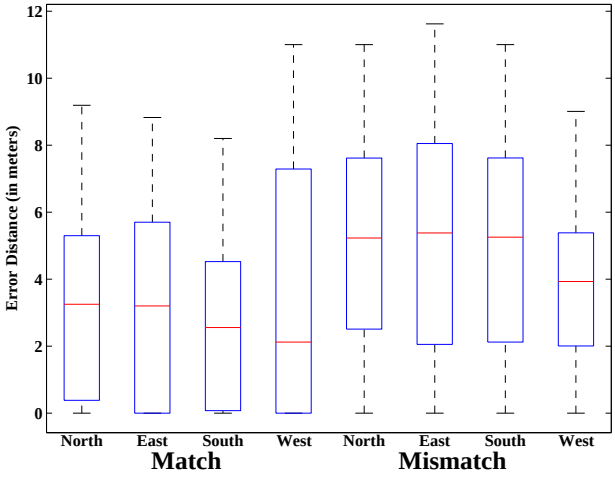

Fig. 4. Box plot of positioning errors under orientation matched and mismatched conditions.

based on RSSs without the assistance of orientation information.

Fig. 4 shows a box plot of the statistical positioning errors in orientation match and mismatch conditions in the fingerprinting system. Each boxs red line represents the median, the blue boxes represent the 25-th and 75-th percentile values, and the dashed lines represent the maximum and minimum value. In this experiment, the term "match" means that both testing and training data are measured in the same user orientation. By contrast, "mismatch" means that the testing data are measured from orientations different from which the training data were measured. For example, the first box for the mismatch condition indicates that the training data are measured from the north, and the testing data are measured from three orientations: east, south and west. Fig. 4 shows that a match between the testing and training orientation is desirable for minimizing the positioning error in a fingerprinting-based location system. By contrast, the performance degrades when the orientation differs between the testing phase and the training phase. In the match condition, the median error was approximately 2.1 to 3 m, whereas that of the mismatch condition increased to 4 to 5.3

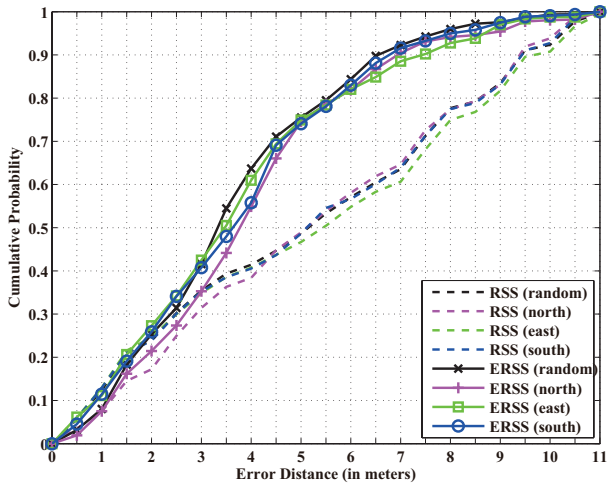

Fig. 5. Cumulative positioning error distribution under the orientation mismatched condition (the orientation of training data is west).

m. Numerical results showed that, in mismatched conditions, the performance of the median positioning error degraded 43.91% on average. These results verify that the mismatch orientation easily influences the positioning accuracy, because the RSS patterns did not match in this scenario.

Fig. 5 displays the cumulative positioning error of the RSS and the Gaussian equalized RSS (ERSS) in the condition of orientation mismatch. In this experiment, the training data were measured from the west whereas the testing data were measured from four distinct directions, north, east, south, and random. This figure shows that the proposed approach outperformed the original method under various mismatch conditions. In this mismatched orientation, the 67-th percentile localization error of the proposed algorithm remained below 4.5 m, whereas that of the RSS increased to 7 m. The proposed algorithm, based on the ERSS, improved the performance of the raw RSS by approximately 28.84% in all cases. Fig. 6 shows the cumulative positioning error under an alternative orientation mismatched condition, where the training data were measured from the north and the testing data was measured from east, south, west, and random. According to Fig. 6, ERSS evidently enhanced the robustness, and the accuracy within 4 m is improved from 48.75% to 79.12%. The results generally agree well with Fig. 5, indicating that the proposed algorithm is capable of achieving robust location estimation, even when orientation is mismatched, by equalizing the temporal-spatial radio power.

Finally, the proposed algorithm is compared with four traditional approaches for addressing the problem of orientation variation: the compass-assisted method [50], [51], the orientation classifier [56], the compressive sensing [53], [54] and the radio map filtering methods [52]. The compass-assisted approach involves the assumption that both the device and radio map contain real-time orientation information and estimating the testing measurement according to the orientation-matched radio map only. Thus, this approach can be regarded as a perfect match case. The orientation classifier estimates the user's orientation according to the moving trajectory and

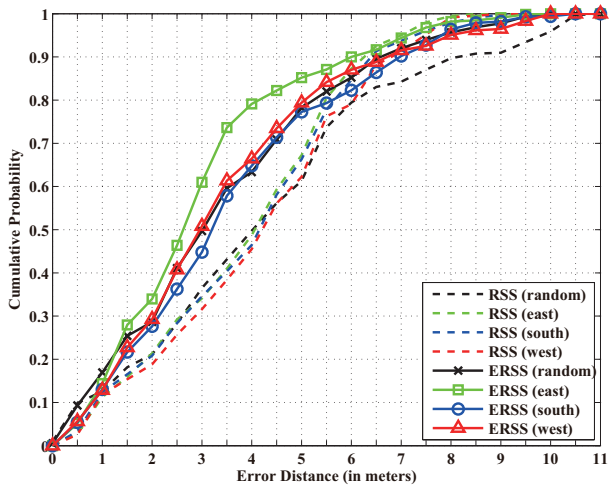

Fig. 6. Cumulative positioning error distribution under an alternative orientation mismatched condition (the orientation of training data is north).

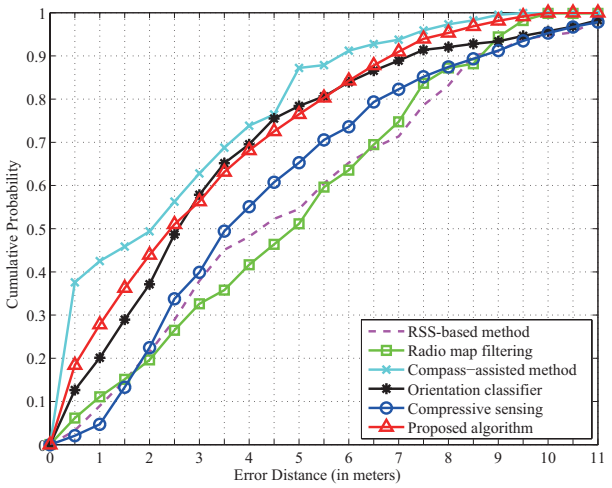

Fig. 7. Performance comparison between different positioning algorithms.

varying RSSs based on the assumption that a user moves in a constant direction at a constant speed. When implementing the orientation classifier, this study assumed a 75% accuracy of estimated direction. The compressive sensing approach combines affinity propagation to improve the positioning accuracy, where the real-time orientation information can be ignored. In this method, we set the number of clusters to 5 and the reduced dimension to 10. The radio map filtering approach removes incompatible RSS samples during the offline and online phase We have implemented these methods and compared the positioning accuracy in a mismatch scenario. Note that, although compressive sensing and radio map filtering are robust to orientation mismatch, they are still based on an extended orientation-aware radio map (i.e., assume the availability of digital compasses during the offline and online phase).

Fig. 7 shows a comparison of the positioning accuracy of various algorithms in a mismatch scenario, where the errors are cumulated from all mismatch conditions and the orientation information of radio map is not given. This figure indicates the effectiveness of the orientation classifier approach. Compared with the traditional RSS method, which is easily influenced by the user orientation, the orientation classifier improved the median error by 38.34%. The compass-assisted approach achieved the most favorable performance, reducing the median error by 51.43% compared with the RSS. This is because the location is accurately estimated according to the orientation-matched radio map. This figure shows that the radio map filtering does not provide significant improvement, as compared to RSS-based method. This is because probabilistic schemes are based on the statistics of the samples, and sufficient number of samples are required to estimate the model parameters. This result agrees well with that in [52]. Next, the result indicates the effectiveness of the compressive sensing approach. This may be that the clustering method reduces the large error, as fewer reference locations are considered. More importantly, Fig. 7 shows that the proposed algorithm provided better performance compared with the orientation classifier, and even comparable accuracy to the compass-assisted method. The result again verified that the ERSS is a robust positioning characteristic. The advantage of the proposed algorithm is that no assumptions are made regarding the orientation process, which is difficult to model because of the random user behavior. Moreover, unlike traditional methods, which require assistance from a digital compass, the proposed algorithm does not require additional hardware and orientation information from radio map .

C. Variation of Reference Distributions

In this section, we performed extra experiments to evaluate the improvement of the proposed algorithm using different reference distributions. We estimated the reference distribution through the training temporal-spatial radio map instead of using Gaussian to perform HEQ. Compared to Gaussianization, the advantage of this approach is that only the testing RSSs are required to be transformed. Tables I and II report five error measures numerically including average, 50%, 67%, 90% percentile errors, and STD (standard deviation) in two mismatch conditions, where ref-G and ref-T indicate the reference distribution is obtained, respectively, by Gaussianization and training data. The experimental setup in Tables I and II is the same as that in Fig. 5 and Fig. 6, respectively.

Both tables show that, no matter what reference distributions the proposed algorithm uses, ERSS still maintained robustness superior to that of RSS. This again demonstrates the effectiveness of the proposed mechanism. Nevertheless, we discover that the performance slightly differs in different scenarios. For example, Tab. II shows that the selection of training data as reference given better results than Gaussian for localization. It seems intuitive because the distribution is empirically calculated using additional information from radio map. However, in Tab. I, Gaussianization outperforms the training data reference when the testing orientations are east and south. This is because the estimated probabilistic distribution is susceptible to data variation. Changing the orientation of training data may introduce bias or errors in the global statistic, making precise distribution estimation difficult. Another critical issue is the amount of training data from radio

TABLE I
FIVE POSITIONING ERROR MEASURES (IN METERS) FOR DIFFERENT ORIENTATION (TRAINING: WEST).

Testing: north					
Methods\Performance	Average	50^{th}	67^{th}	90^{th}	STD
RSS-based method	5.22	5.22	7.15	9.41	3.04
ERSS-based (Ref-G)	3.95	3.69	4.52	6.89	2.27
ERSS-based (Ref-T)	3.75	3.58	4.50	6.72	2.13
Testing: east					
Methods\Performance	Average	50^{th}	67^{th}	90^{th}	STD
RSS-based method	5.23	5.37	7.38	9.50	3.35
ERSS-based (Ref-G)	3.73	3.46	4.27	7.39	2.42
ERSS-based (Ref-T)	3.88	3.72	4.69	6.67	2.13
Testing: south					
Methods\Performance	Average	50^{th}	67^{th}	90^{th}	STD
RSS-based method	5.10	5.25	7.28	9.48	3.23
ERSS-based (Ref-G)	3.74	3.60	4.29	6.71	2.26
ERSS-based (Ref-T)	3.86	3.72	4.77	7.05	2.20
Testing: random					
Methods\Performance	Average	50^{th}	67^{th}	90^{th}	STD
RSS-based method	5.09	5.19	7.20	9.42	3.24
ERSS-based (Ref-G)	3.64	3.26	4.18	6.51	2.15
ERSS-based (Ref-T)	3.79	3.60	4.38	7.43	2.44

TABLE II
FIVE POSITIONING ERROR MEASURES (IN METERS) FOR DIFFERENT ORIENTATION (TRAINING: NORTH).

Testing: east					
Methods\Performance	Average	50^{th}	67^{th}	90^{th}	STD
RSS-based method	3.83	4.03	5.00	6.15	1.90
ERSS-based (Ref-G)	2.93	2.59	3.23	5.99	1.96
ERSS-based (Ref-T)	2.59	2.31	3.23	6.27	2.27
Testing: south					
Methods\Performance	Average	50^{th}	67^{th}	90^{th}	STD
RSS-based method	3.90	4.10	5.04	6.39	2.02
ERSS-based (Ref-G)	3.53	3.17	4.11	6.99	2.24
ERSS-based (Ref-T)	2.49	2.37	3.12	5.82	2.34
Testing: west					
Methods\Performance	Average	50^{th}	67^{th}	90^{th}	STD
RSS-based method	4.04	4.12	5.09	6.67	2.02
ERSS-based (Ref-G)	3.37	2.95	4.00	6.67	2.24
ERSS-based (Ref-T)	2.41	2.23	3.00	6.09	2.41
Testing: random					
Methods\Performance	Average	50^{th}	67^{th}	90^{th}	STD
RSS-based method	4.18	4.03	5.20	8.03	2.72
ERSS-based (Ref-G)	3.34	3.00	4.21	6.59	2.28
ERSS-based (Ref-T)	2.42	2.24	3.05	6.14	2.37

map. When the target indoor environment is large, the amount of estimation samples may be insufficient for a reliable histogram computation. As mentioned, the data-driven reference distribution could enhance the robustness against orientation mismatch. Nevertheless, we note that, Gaussianization is a safer approach to accommodate as much data variation as possible in the face of limited training data, unknown indoor environments and training orientation.

D. Analysis of Results

To provide insight into the proposed algorithm, how the ERSS compensates for the effect of orientation mismatch in location estimation is analyzed in this section. Fig. 8 shows the original Wi-Fi RSS probability distributions, which were

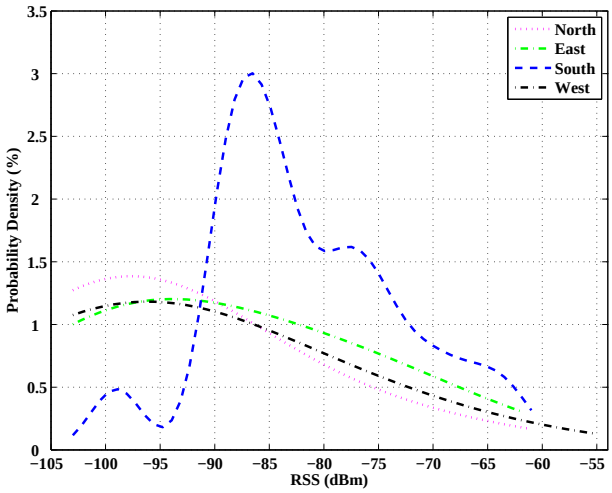

Fig. 8. The impact of diverse orientations on the probability density of temporal-spatial RSS samples at a fixed reference location.

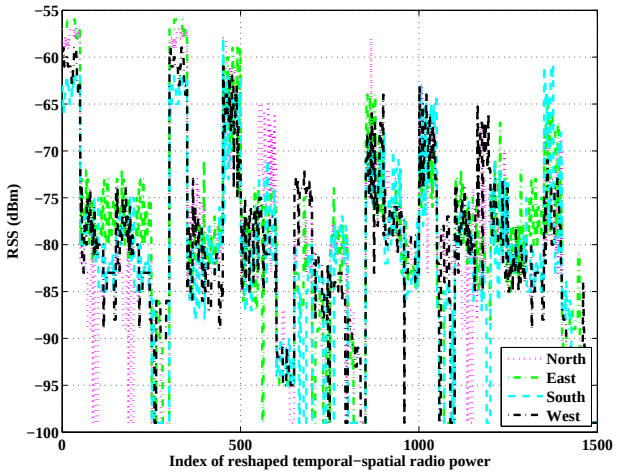

Fig. 9. The impact of diverse orientations on the absolute RSS values of the reshaped temporal-spatial vector (Eq. 9) at a fixed reference location.

estimated according to the measurements from 1500 temporal-spatial signals (50 temporal samples from 30 APs) at a specific reference location. This figure shows that the diverse orientations severely affect the probability distributions of the Wi-Fi radio power. In the proposed algorithm, the effect of the orientation is assumed to be a certain transformation of the RSS representation space, incurring a considerable mismatch problem when training and locating orientations differ. Fig. 8 verifies this assumption. This observation is generally consistent for all reference locations. Fig. 9 shows the absolute RSS values of the reshaped vector in Eq. 9. This figure shows how the multidimensional RSSs from four orientations change over time. Similarly, this figure shows that a substantial influence resulted from the different orientations. This verifies the effect of orientation on measuring Wi-Fi radio, and the mismatch causes determining the location based on training RSS patterns to be difficult when using the fingerprinting-based system.

Fig. 10 shows an equalization case, where the testing RSS measured from the E are transformed such that their cumulative histogram matches that of the reference training

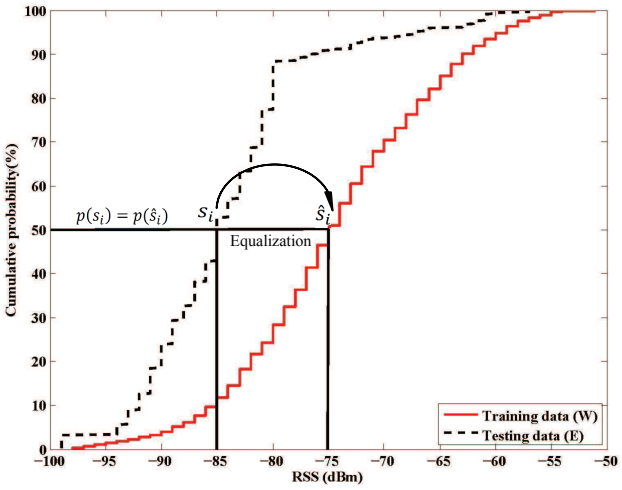

Fig. 10. An equalization case. The testing RSSs measured from the E are transformed such that their cumulative histogram matches that of the reference training data measured from the W.

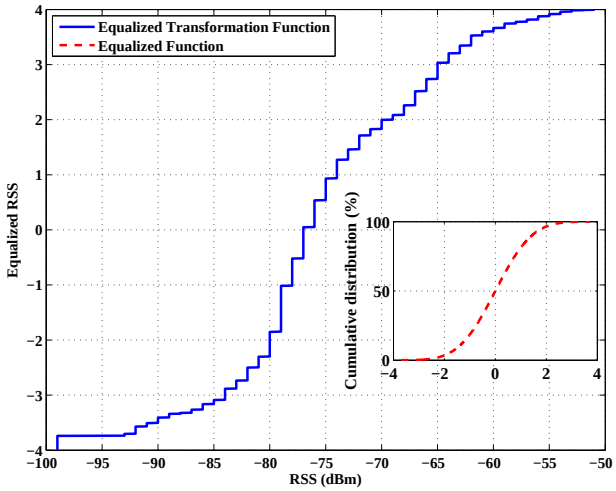

Fig. 11. An example of the transformation function to equalize RSS and the reference histogram function.

data measured from the W. For example, the proposed algorithm changes the RSS values -85 into -75 dBm in Fig. 10 because the same cumulative probability 50% is presented in original and equalized domain, respectively. Note that in this case, the positioning error using RSS is 6.84 m on average under orientation mismatch conditions whereas it was reduced to 2.84 m using the equalized RSS. That means that the impact of orientation was significantly alleviated through the equalization process. In other words, the proposed algorithm compensates for variation in user orientations, which distorts the RSS space. Similar plots can be observed for testing data at different locations and orientations, and only a typical case is shown in Fig. 10 because of space limitations.

Fig. 11 shows the transformations obtained in Gaussianization case used to convert the original RSS histograms into the reference histogram, by using the proposed algorithm. This figure shows that, in this case, the RSS values ranging from -50 to -100 dBm were transformed into an equalized version ranging from -4 to +4. When a Gaussian was used as the reference distribution, the corresponding reference histogram was easily obtained and is also depicted in Fig. 11. After the equalization, the histograms of the transformed RSS representations are shown in Fig. 12. This figure shows that the transformed RSSs approximate the reference probability distribution and indicates that the impact of orientation on the distribution was considerably alleviated, as indicated in Figs. 8 and 9. When an orientation mismatch occurs between training and locating conditions, the proposed algorithm normalizes all moments of RSSs distribution to those of the reference distributions. Note that although the absolute RSS vales were equalized, the relative information between the multi-dimensional RSSs was still preserved for localization. Finally, Fig. 13 shows the temporal-spatial trajectory of the ERSSs. Compared with Fig. 9, Fig. 13 shows that the orientation mismatch was substantially reduced. The experiments and analysis reveal the effectiveness of the proposed algorithm in providing robust indoor Wi-Fi localization in the presence of orientation mismatch.

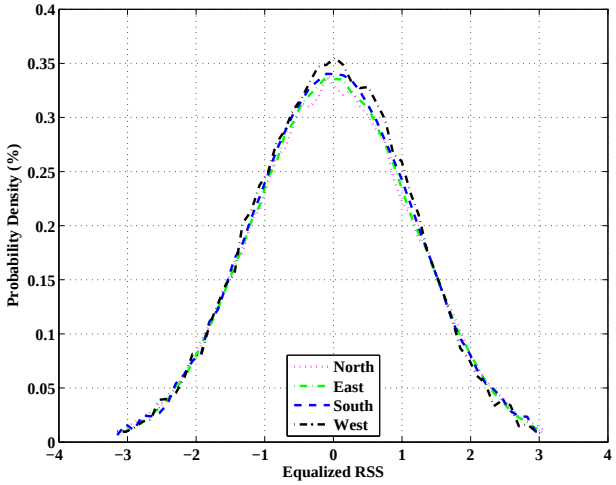

Fig. 12. The impact of diverse orientations on the probability density of equalized Gaussian RSSs at a fixed reference location.

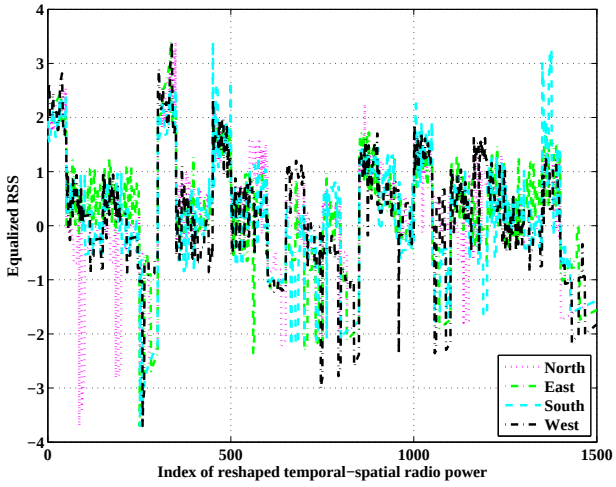

Fig. 13. The equalized RSSs of the reshaped temporal-spatial vector at a fixed reference location.

IV. Conclusion

This study proposes a novel approach based on HEQ to compensate for an orientation mismatch in robust Wi-Fi localization. By transforming the temporal-spatial radio signal strength into a reference histogram, the proposed algorithm effectively prevents the performance degradation under orientation mismatch conditions. Specifically, HEQ is applied to each component of temporal-spatial radio to improve the robustness of indoor localization systems. The proposed approach is conceptually simple and easy to implement in practical applications. The advantages of the proposed algorithm are that it does not involve assumptions regarding the random user behavior, and does not require embedding a digital compass in mobile devices. The experiments, conducted in an indoor Wi-Fi environment, confirm the superiority of the proposed algorithm in orientation mismatch compensation. Results show that the proposed algorithm outperforms the orientation classifier method and provides a comparable positioning accuracy to that of the compass-assisted approach.

Acknowledgment

The authors would like to thank the National Science Council for providing financial support (NSC101-2221-E-155-003 and NSC102-2221-E-155-006-MY3).

References

[1] Y. Gu, A. Lo, and I. Niemegeers, "A survey of indoor positioning systems for wireless personal networks," *IEEE Transactions on Communications Surveys Tutorials*, vol. 11, no. 1, pp. 13–32, 2009.

[2] J. Perez-Ramirez, D. Borah, and D. Voelz, "Optimal 3-D landmark placement for vehicle localization using heterogeneous sensors," *IEEE Transactions on Vehicular Technology*, vol. 62, pp. 2987–2999, Sept 2013.

[3] J. Sun, X. Zhu, C. Zhang, and Y. Fang, "Rescueme: Location-based secure and dependable VANETs for disaster rescue," *IEEE Journal on Selected Areas in Communications*, vol. 29, pp. 659–669, March 2011.

[4] K. Yu and E. Dutkiewicz, "Geometry and motion-based positioning algorithms for mobile tracking in NLOS environments," *IEEE Transactions on Mobile Computing*, vol. 11, pp. 254–263, Feb 2012.

[5] M. B. Kjærgaard, "A taxonomy for radio location fingerprinting," LoCA, pp. 139–156, Springer-Verlag, 2007.

[6] J. Teng, H. Snoussi, C. Richard, and R. Zhou, "Distributed variational filtering for simultaneous sensor localization and target tracking in wireless sensor networks," *IEEE Transactions on Vehicular Technology*, vol. 61, pp. 2305–2318, Jun 2012.

[7] I. Sharp and K. Yu, "Enhanced least-squares positioning algorithm for indoor positioning," *IEEE Transactions on Mobile Computing*, vol. 12, pp. 1640–1650, Aug 2013.

[8] P. Bahl and V. Padmanabhan, "RADAR: an in-building RF-based user location and tracking system," in *INFOCOM*, vol. 2, pp. 775–784, 2000.

[9] M. Youssef and A. Agrawala, "The Horus location determination system," *Wireless Netw.*, vol. 14, pp. 357–374, 2008.

[10] T. Lin, S. Fang, W. Tseng, C. Lee, and J. Hsieh, "A group-discrimination-based access point selection for WLAN fingerprinting localization," *IEEE Transactions on Vehicular Technology*, vol. PP, no. 99, pp. 1–1, 2014.

[11] S.-H. Fang, C.-H. Wang, T.-Y. Huang, C.-H. Yang, and Y.-S. Chen, "An enhanced ZigBee indoor positioning system with an ensemble approach," *IEEE Communications Letters*, vol. 16, no. 4, pp. 564–567, 2012.

[12] M. Bshara, U. Orguner, F. Gustafsson, and L. Van Biesen, "Fingerprinting localization in wireless networks based on received-signal-strength measurements: A case study on WiMAX networks," *IEEE Transactions on Vehicular Technology*, vol. 59, no. 1, pp. 283–294, 2010.

[13] C. Figuera, J. Rojo-Alvarez, I. Mora-Jimenez, A. Guerrero-Curieses, M. Wilby, and J. Ramos-Lopez, "Time-space sampling and mobile device calibration for WiFi indoor location systems," *IEEE Transactions on Mobile Computing*, vol. 10, no. 7, pp. 913–926, 2011.

[14] L. Liao, W. Chen, C. Zhang, L. Zhang, D. Xuan, and W. Jia, "Two birds with one stone: Wireless access point deployment for both coverage and localization," *IEEE Transactions on Vehicular Technology*, vol. 60, pp. 2239–2252, Jun 2011.

[15] M. Youssef, A. Agrawala, and A. Udaya Shankar, "WLAN location determination via clustering and probability distributions," in *Pervasive Computing and Communications*, pp. 143–150, 2003.

[16] A. Tsui, W.-C. Lin, W.-J. Chen, P. Huang, and H.-H. Chu, "Accuracy performance analysis between war driving and war walking in metropolitan Wi-Fi localization," *IEEE Transactions on Mobile Computing*, vol. 9, no. 11, pp. 1551–1562, 2010.

[17] S.-H. Fang and C.-H. Wang, "A dynamic hybrid projection approach for improved Wi-Fi location fingerprinting," *IEEE Transactions on Vehicular Technology*, vol. 60, no. 3, pp. 1037–1044, 2011.

[18] S.-P. Kuo and Y.-C. Tseng, "Discriminant minimization search for large-scale RF-based localization systems," *IEEE Transactions on Mobile Computing*, vol. 10, no. 2, pp. 291–304, 2011.

[19] S. Coleri Ergen, H. Tetikol, M. Kontik, R. Sevlian, R. Rajagopal, and P. Varaiya, "RSSI-fingerprinting-based mobile phone localization with route constraints," *IEEE Transactions on Vehicular Technology*, vol. 63, pp. 423–428, Jan 2014.

[20] S.-P. Kuo and Y.-C. Tseng, "A scrambling method for fingerprint positioning based on temporal diversity and spatial dependency," *IEEE Transactions on Knowledge and Data Engineering*, vol. 20, no. 5, pp. 678–684, 2008.

[21] H. Shin, Y. Chon, and H. Cha, "Unsupervised construction of an indoor floor plan using a smartphone," *IEEE Transactions on Systems, Man, and Cybernetics, Part C: Applications and Reviews*, vol. 42, no. 6, pp. 889–898, 2012.

[22] A. Bernardos, J. Casar, and P. Tarrio, "Real time calibration for RSS indoor positioning systems," in *IPIN*, pp. 1–7, 2010.

[23] S. Mazuelas, A. Bahillo, R. Lorenzo, P. Fernandez, F. Lago, E. Garcia, J. Blas, and E. Abril, "Robust indoor positioning provided by real-time RSSI values in unmodified WLAN networks," *IEEE Journal of Selected Topics in Signal Processing*, vol. 3, no. 5, pp. 821–831, 2009.

[24] A. Mahtab Hossain, Y. Jin, W.-S. Soh, and H. N. Van, "SSD: A robust RF location fingerprint addressing mobile devices' heterogeneity," *IEEE Transactions on Mobile Computing*, vol. 12, no. 1, pp. 65–77, 2013.

[25] M. B. Kjærgaard, "Indoor location fingerprinting with heterogeneous clients," *Pervasive Mob. Comput.*, vol. 7, pp. 31–43, 2011.

[26] F. Dong, Y. Chen, J. Liu, Q. Ning, and S. Piao, "A calibration-free localization solution for handling signal strength variance," in *MELT*, pp. 79–90, Springer-Verlag, 2009.

[27] Y. Zhang, W. Liu, Y. Fang, and D. Wu, "Secure localization and authentication in ultra-wideband sensor networks," *IEEE Journal on Selected Areas in Communications*, vol. 24, no. 4, pp. 829–835, 2006.

[28] Y. Chen, K. Kleisouris, X. Li, W. Trappe, and R. P. Martin, "A security and robustness performance analysis of localization algorithms to signal strength attacks," *ACM Trans. Sen. Netw.*, vol. 5, pp. 2:1–2:37, Feb. 2009.

[29] M. Li, X. Jiang, and L. Guibas, "Fingerprinting mobile user positions in sensor networks: Attacks and countermeasures," *IEEE Transactions on Parallel and Distributed Systems*, vol. PP, no. 99, p. 1, 2011.

[30] S.-H. Fang, C.-C. Chuang, and C. Wang, "Attack-resistant wireless localization using an inclusive disjunction model," *IEEE Transactions on Communications*, vol. 60, no. 5, pp. 1209–1214, 2012.

[31] Y. Chen, J. Yang, W. Trappe, and R. Martin, "Detecting and localizing identity-based attacks in wireless and sensor networks," *IEEE Transactions on Vehicular Technology*, vol. 59, no. 5, pp. 1–1, 2010.

[32] S. Medawar, P. Handel, and P. Zetterberg, "Approximate maximum likelihood estimation of rician K-Factor and investigation of urban wireless measurements," *IEEE Transactions on Wireless Communications*, vol. 12, no. 6, pp. 2545–2555, 2013.

[33] K. Yu and E. Dutkiewicz, "NLOS identification and mitigation for mobile tracking," *IEEE Transactions on Aerospace and Electronic Systems*, vol. 49, pp. 1438–1452, July 2013.

[34] S.-H. Fang, T.-N. Lin, and K.-C. Lee, "A novel algorithm for multipath fingerprinting in indoor WLAN environments," *IEEE Transactions on Wireless Communications*, vol. 7, no. 9, pp. 3579–3588, 2008.

[35] O. Bialer, D. Raphaeli, and A. Weiss, "Maximum-likelihood direct position estimation in dense multipath," *IEEE Transactions on Vehicular Technology*, vol. 62, pp. 2069–2079, Jun 2013.

[36] L. Mihaylova, D. Angelova, D. Bull, and N. Canagarajah, "Localization of mobile nodes in wireless networks with correlated in time measurement noise," *IEEE Transactions on Mobile Computing*, vol. 10, no. 1, pp. 44–53, 2011.

[37] K. Yu and Y. Guo, "Statistical NLOS identification based on AOA, TOA, and signal strength," *IEEE Transactions on Vehicular Technology*, vol. 58, pp. 274–286, Jan 2009.

[38] W. Li, Y. Jia, J. Du, and J. Zhang, "Distributed multiple-model estimation for simultaneous localization and tracking with NLOS mitigation," *IEEE Transactions on Vehicular Technology*, vol. 62, pp. 2824–2830, July 2013.

[39] T. Roos, P. Myllymaki, and H. Tirri, "A statistical modeling approach to location estimation," *IEEE Transactions on Mobile Computing*, vol. 1, no. 1, pp. 59–69, 2002.

[40] S. Gezici, "A survey on wireless position estimation," *Wireless Personal Communications*, vol. 44, pp. 263–282, 2008.

[41] T. Garcia-Valverde, A. Garcia-Sola, J. Botia, and A. Gomez-Skarmeta, "Automatic design of an indoor user location infrastructure using a memetic multiobjective approach," *IEEE Transactions on Systems, Man, and Cybernetics, Part C: Applications and Reviews*, vol. 42, no. 5, pp. 704–709, 2012.

[42] H. Liu, Y. Gan, J. Yang, S. Sidhom, Y. Wang, Y. Chen, and F. Ye, "Push the limit of WiFi based localization for smartphones," in *Mobicom*, pp. 305–316, 2012.

[43] S.-H. Fang and T.-N. Lin, "Accurate WLAN indoor localization based on RSS fluctuations modeling," in *IEEE International Symposium on Intelligent Signal Processing*, pp. 27–30, 2009.

[44] N. Ghaboosi and A. Jamalipour, "Location estimation using geometry of overhearing under shadow fading conditions," *IEEE Transactions on Wireless Communications*, vol. 11, no. 11, pp. 4140–4149, 2012.

[45] H. Liu, H. Darabi, P. Banerjee, and J. Liu, "Survey of wireless indoor positioning techniques and systems," *IEEE Transactions on Systems, Man, and Cybernetics, Part C: Applications and Reviews*, vol. 37, no. 6, pp. 1067–1080, 2007.

[46] B. Roberts and K. Pahlavan, "Site-specific RSS signature modeling for WiFi localization," in *GLOBECOM*, pp. 1–6, 2009.

[47] S.-H. Fang, C.-H. Wang, S.-M. Chiou, and P. Lin, "Calibration-free approaches for robust Wi-Fi positioning against device diversity: A performance comparison," in *Vehicular Technology Conference*, pp. 1–5, 2012.

[48] A. M. Ladd, K. E. Bekris, A. Rudys, G. Marceau, L. E. Kavraki, and D. S. Wallach, "Robotics-based location sensing using wireless ethernet," in *Mobile computing and networking*, pp. 227–238, 2002.

[49] K. Kaemarungsi and P. Krishnamurthy, "Properties of indoor received signal strength for WLAN location fingerprinting," in *Mobile and Ubiquitous Systems: Networking and Services*, pp. 14–23, 2004.

[50] T. King, S. Kopf, T. Haenselmann, C. Lubberger, and W. Effelsberg, "COMPASS: A probabilistic indoor positioning system based on 802.11 and digital compasses," in *WiNTECH*, pp. 34–40, 2006.

[51] D. Sanchez, J. Quinteiro, P. Hernandez-Morera, and E. Martel-Jordan, "Using data mining and fingerprinting extension with device orientation information for WLAN efficient indoor location estimation," in *Conference on Wireless and Mobile Computing, Networking and Communications*, pp. 77–83, 2012.

[52] A. Papapostolou and H. Chaouchi, "Orientation-based radio map extensions for improving positioning system accuracy," in *International Conference on Wireless Communications and Mobile Computing: Connecting the World Wirelessly*, pp. 947–951, ACM, 2009.

[53] C. Feng, W. Au, S. Valaee, and Z. Tan, "Orientation-aware indoor localization using affinity propagation and compressive sensing," in *IEEE International Workshop on Computational Advances in Multi-Sensor Adaptive Processing*, pp. 261–264, 2009.

[54] C. Feng, W. Au, S. Valaee, and Z. Tan, "Received-signal-strength-based indoor positioning using compressive sensing," *IEEE Transactions on Mobile Computing*, vol. 11, pp. 1983–1993, Dec 2012.

[55] B. J. Frey and D. Dueck, "Clustering by passing messages between data points," *Science*, vol. 315, p. 2007, 2007.

[56] I.-E. Liao and K.-F. Kao, "Enhancing the accuracy of WLAN-based location determination systems using predicted orientation information," *Information Sciences*, vol. 178, no. 4, pp. 1049 – 1068, 2008.

[57] J. C. Russ, *Image Processing Handbook*. 1995.

[58] A. De la Torre, A. Peinado, J. Segura, J. Perez-Cordoba, M. Benitez, and A. Rubio, "Histogram equalization of speech representation for robust speech recognition," *IEEE Transactions on Speech and Audio Processing*, vol. 13, no. 3, pp. 355–366, 2005.

[59] J. Li, L. Deng, Y. Gong, and R. Haeb-Umbach, "An overview of noise-robust automatic speech recognition," *IEEE/ACM Transactions on Audio, Speech, and Language Processing*, vol. 22, pp. 745 – 777, April 2014.

[60] Dharanipragada, Satya, and M. Padmanabhan, "A nonlinear unsupervised adaptation technique for speech recognition," in *INTERSPEECH*, pp. 556–559, 2000.